

PAPER • OPEN ACCESS

## Carbon Dioxide Adsorption on MOF-199 Metal-Organic Framework at High Pressure

To cite this article: Rana Th. A. Alrubaye and Huda M. Kareem 2019 *IOP Conf. Ser.: Mater. Sci. Eng.* **557** 012060

View the [article online](#) for updates and enhancements.

# Carbon Dioxide Adsorption on MOF-199 Metal-Organic Framework at High Pressure

Rana Th. A. Alrubaye<sup>1,2</sup>, Huda M. Kareem<sup>1</sup>

<sup>1</sup> Chemical Engineering Department, College of Engineering, University of Baghdad, Jadrai, Baghdad, Iraq

<sup>2</sup> Corresponding author. Email : Alrubaye.rana@gmail.com

**Abstract.** MOFs have considered as promising materials for CO<sub>2</sub> adsorption due to their excellent chemical stability, large pore volume, and high surface area. In this study, MOF-199 has been synthesized using the solvent-thermal method with focusing on the significant parameters that affecting the structure of the MOF-199 (solvent, synthesis time, and temperature). Produced MOF-199 samples were characterized by electron scan microscope, X-ray diffraction, and microporosimetric analysis. High crystallinity degree and high surface area were found at 1:1 of the H<sub>2</sub>O: C<sub>2</sub>H<sub>5</sub>OH (within the solvents range from 1:1 to 1:2 ratios), whereas the changing of the synthesis duration from 18 to 48 h, and synthesis temperatures from 40 to 140 °C have revealed that the best synthesis conditions are 100 °C for 48 h. The appropriate activation condition has been determined to be 60 °C for 16 h. For CO<sub>2</sub> adsorption isotherms on MOF-199 were at a temperature (36, 40, 60, and 70) °C and pressure range (0-5) bar using a volumetric technique. Temkin, Freundlich and Langmuir isotherm models have been used to analyze the equilibrium data. This research presents the effect of significant parameters on the synthesis of MOF-199 to understand their influence on the formation of MOF structures and the CO<sub>2</sub> adsorption capacities.

**Keywords:** MOF-199, CO<sub>2</sub> adsorption, synthesis temperature and time

## 1. Introduction

MOFs are new crystalline coordination polymers that have investigated in the past two decades [1]. These new materials are ordered porous solids that are forming by soluble complexes consist of inorganic particles or ion clusters and organic linkers, then self-assemble into frameworks. The formation of MOFs has a significant advantage of designing and tailoring the structure and sizes of pores in the framework, and metal ions and organic ligands selection could achieve that. Different MOFs structures can be obtained by varying the coordination environments of the central metals controlled by the several factors that affecting the synthesis process these factors are the solvent, synthesis temperature and time [2].

Cui [1] experiments revealed that the process of solvation and organize formation for MOFs of different environments for self-assembly could be affected by the water present in a mixed solvent system. Therefore dimensionality of the final structures seemed to be tuned by varying C<sub>2</sub>H<sub>5</sub>OH:H<sub>2</sub>O ratio. The effect of the choice of the solvent has been clearly reflected in the obtained structures.

Solvothermal of MOFs offers advantages compared to other structural methods. The synthesis under solvothermal in a closed system at pressures higher than 1atm and a temperature higher than 100 °C will ensure the high solubility of all the reactants and high-quality crystals can be obtained which led to the high crystallization of MOFs [3].



Sarawade et al reported the influence of reaction temperature and time on size, shape, and morphology of MOF microcrystals formed by microwave synthesis. In addition, the higher dimensional MOFs were produced which indicated, the easier deprotonating of the ligand at higher temperatures [4].

The Metal-Organic Frameworks have recently used for numerous applications as promising alternatives for gas separation due to their ease of manipulation in porous structures and flexibility in composition and chemical properties.

MOF-199 is considered as a highly demanding porous material in gas separation and adsorption due to its large pore volume high, high surface area (generally in a range of 600–1600 m<sup>2</sup> g<sup>-1</sup>) and excellent thermal stability. MOF-199 is one of the most widely studied MOF materials as a CO<sub>2</sub> capturing agent. Researcher reported that the uptake capacity for CO<sub>2</sub> of MOF-199 (at 1 atm and 220 °C) was 69 ml g<sup>-1</sup> [5], and the capacity of the CO<sub>2</sub> uptake at high-pressure ranges at 25 °C from 8 to 11 mmol g<sup>-1</sup> as examined by [3].

In this study, the synthesis of the highly porous metal-organic framework MOF-199 is reported. The effect of parameters such as solvent volume, synthesis temperature and reaction time were studied. The CO<sub>2</sub> storage capacity of the material and static adsorption isotherms on MOF-199 was also investigated.

## 2. Materials and Methods

### 2.1. Materials

MOF-199 was synthesized using copper (II) nitrate trihydrate [Cu(NO<sub>3</sub>)<sub>2</sub>·3H<sub>2</sub>O, 99%] and benzene-1,3,5 tricarboxylic acid (BTC, 95%) obtained from Sigma Aldrich. Absolute ethanol (C<sub>2</sub>H<sub>5</sub>OH) from Fisher scientific.

### 2.2. Solvent-thermal synthesis of MOF-199

MOF-199 was synthesized following Schlichte's method [6] using solvent-thermal synthesis and BTC (0.42 g) dissolved in 24 ml of 1:1 or 2:1 C<sub>2</sub>H<sub>5</sub>OH:H<sub>2</sub>O solvent ratio. The prepared mixture was stirred until a clear solution was obtained (10 min). Then Cu(NO<sub>3</sub>)<sub>2</sub>·3H<sub>2</sub>O (0.875 g) was added to the mixture and stirred thoroughly for another 10 min. Once completely dissolved reached in the solvent, the resulting blue solution was transferred to a 50 ml stainless steel Teflon lined autoclave and heated to a specific temperature at specific crystallization time (see Table 1). In order to investigate the effect of the operation conditions changing on the solve-thermal synthesis of MOF-199 the heating temperature was changed from 40 to 140 °C and the reaction time was varied from 18 to 48 h. Then, the reactor was cooled to room temperature, and a blue crystalline powder was formed. The powder was then filtered and washed thoroughly with a 60 ml mixture of water and ethanol (1:1). The product was finally activated under vacuum at 60°C for 21 h and stored in closed vials at 60°C in oven for further experiments.

**Table 1.** Summary of the MOF-199 samples synthesized

Sample	Time h	Temperature °C	C <sub>2</sub> H <sub>5</sub> OH:H <sub>2</sub> O ratio
S1	18	100	1:1
S2	24	100	1:1
S3	30	100	1:1
S4	48	40	1:1
S5	48	85	1:1
S6	48	100	1:1
S7	48	140	1:1
S8	48	100	2:1

### 2.3. Characterization of MOF-199

scanning electron microscope (SEM) was carried out using FEI Quanta 200 ESEM equipment with a high voltage mode of 20 kV to obtain MOF-199 synthesized samples morphology. All samples were characterized to confirm the formation of MOF-199 using powder X-ray diffraction (XRD), which

was achieved by a Rigaku Miniflex diffractometer (CuK $\alpha$  radiation, 30 kV, 15 mA,  $\lambda = 1.5406 \text{ \AA}$ ) using a step-scan mode ( $0.03^\circ$  per step) with a range of  $5^\circ < 2\theta < 46^\circ$ . ASAP 2020 Micromeritics instrument was used for N<sub>2</sub> adsorption/desorption cycles, which achieved by Microporosimetric analysis at 77 K, the surface area was determined using the Brunauer- Emmett-Teller (BET) method. All synthesized samples were degassed at 180 °C for 3 h prior to characterization.

#### 2.4. CO<sub>2</sub> isotherms adsorption

The CO<sub>2</sub> adsorption capacity of MOF-199 was investigated using pressure swing adsorption (PSA). The necessary steps in the pressure swing adsorption were evaluated using an experiential apparatus, which was designed for wide-range conditions (high pressure, temperature, flow rate, adiabatic, etc.). The apparatus was automated and controlled, with the only manual operations being the analysis of samples and the recording of flow rates and pressure as shown in Figure 1

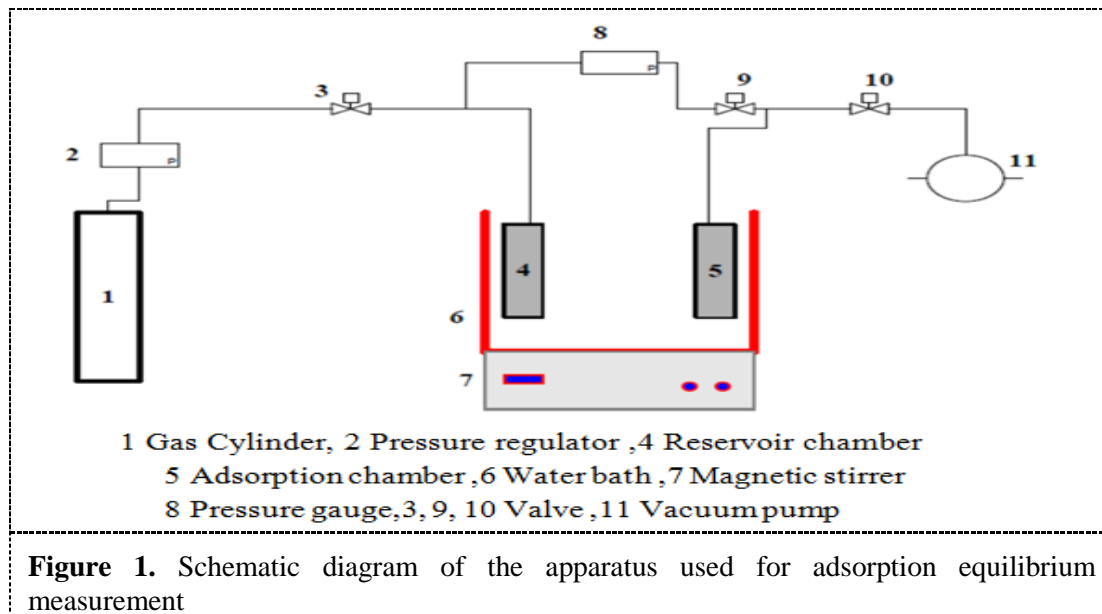


**Figure 1.** Schematic diagram of the apparatus used for adsorption equilibrium measurement

The volume of the whole system was measured manometrically using N<sub>2</sub> gas. A weighted sample had been regenerated in the adsorption column by degasifying the sample to a pressure less than 3 bar for an overnight prior to each test. After the MOFs had been regenerated, the heating was on, and a stream of CO<sub>2</sub> was passed through the apparatus for about 120 min or until the whole adsorbent bed reaches the specific temperature. Simultaneously, the gage pressure was monitored. The amount of gas adsorbed at equilibrium was determined from Eq(1):

$$q = \frac{(c_{ri} - c_{rf})V_r - C_{rf} \epsilon V_a}{W} \quad (1)$$

$q$  is adsorbent loading at equilibrium (mmol/g),  $V$  is volume (l),  $C$  is concentration (mmol/l),  $f$  is overall bed void fraction, and  $W$  is the weight of the adsorbent in the absorber vessel (g), the subscripts  $r$ ,  $a$ ,  $i$  and refer to reservoir, adsorbed vessel, initial and final condition respectively,  $C_e$  ( $C_{ri} - C_{rf}$ ) concentration equilibrium.  $T_c$  critical temperature of CO<sub>2</sub> ( $31^\circ\text{C}$ ),  $P_c$  critical pressure of CO<sub>2</sub> (73 atm),  $R$  gas constant (8.314 L.Kpa/ mol. K),  $T$  is Temperature use for adsorption.  $C_{ri}$  and  $C_{rf}$  where calculate from equation of real gases :

$$P V = Z n R T \quad (n/v=C)$$

$$C_{ri} = \frac{P_i}{Z_i R T} \quad (2)$$

$$C_{rf} = \frac{Pf}{Z_f R T} \quad (3)$$

Z compressibility factor of feed and out gases may be estimated according to the generalized equation :

$$Z = 1 + \frac{BP}{RT} \quad (4)$$

The coefficient of B where calculated by:

$$\frac{BP_c}{RT_c} = B + \omega B' \quad (5)$$

The coefficient of B and B' may be estimated as follows:

$$B = 0.083 - \frac{0.422}{T_r^{1.6}} \quad (6)$$

$$B' = 0.139 - \frac{0.172}{T_r^{1.2}} \quad (7)$$

$T_r = T/T_c$

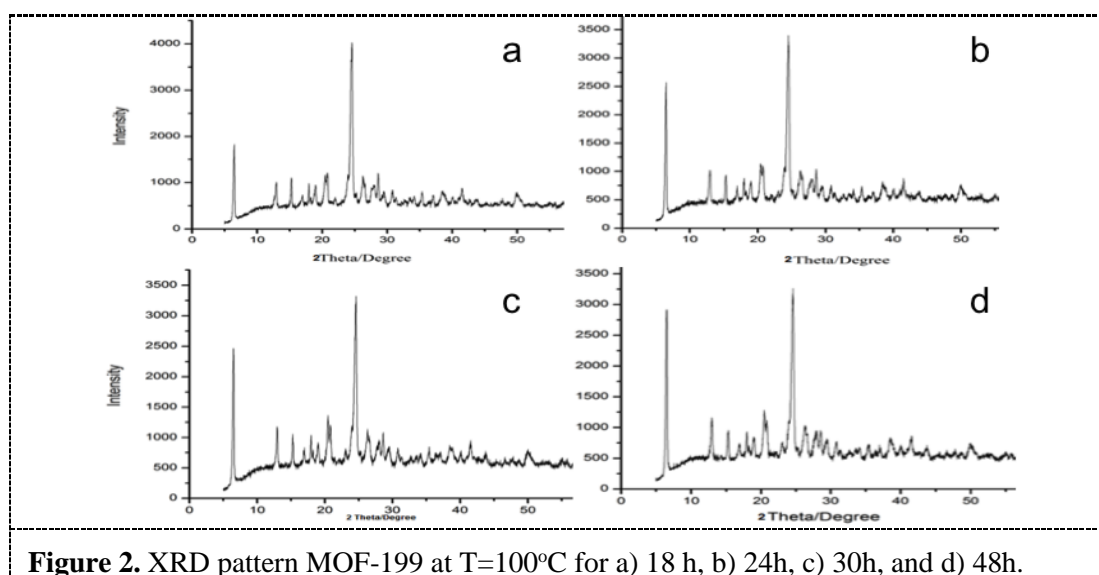
### 3. Results and discussion

#### 3.1. Characterization of MOF-199

All collected XRD diffraction data of synthesized samples, which are shown in Figures 2 to 4, are consistent with those reported for the typical XRD pattern of MOF-199 (Nobar,2012). Formation of large size crystals can explain the significant high intensity of peaks in the XRD pattern, however, in this study, it could be related to the lower content of water inside the pore of the synthesized MOF. And that because of the sample immediately was inserting inside the analysis chamber after the drying process at 110 °C The XRD pattern of MOF-199 exemplifies its crystalline phase with characteristic peaks at  $2\theta \approx 6.5^\circ, 9.5^\circ, 11.5^\circ,$  and  $13.4^\circ$ , which were confirming the formation of MOF-199 crystalline phase. The  $\text{Cu}_2\text{O}$  characteristic diffraction peaks were at  $2\theta \approx 36.4^\circ, 42.3^\circ$  and  $43.3^\circ$  [7].

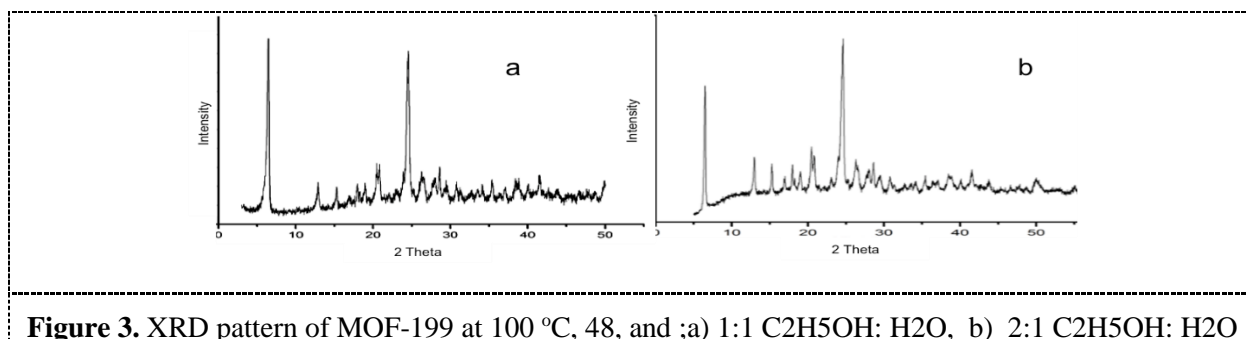
The relative crystallinity of metal-organic frameworks of all synthesized samples was calculated by finding the percentage ratio of the sum of the peak intensities for the synthesized MOF-199 samples and the sum of the peak intensities of the standard MOF-199 [8].

Figure 2. show the effect of the changing the reaction time from 18 to 48 hours at constant synthesis temperature (100°C) and 1:1  $\text{C}_2\text{H}_5\text{OH}:\text{H}_2\text{O}$  solvent ratio on the structure of the synthesized samples (S1, S2, S3 and S4). The formation of MOF-199 is indicated by the appearance of characteristic peaks after 18 hours at reaction temperature 100 °C.



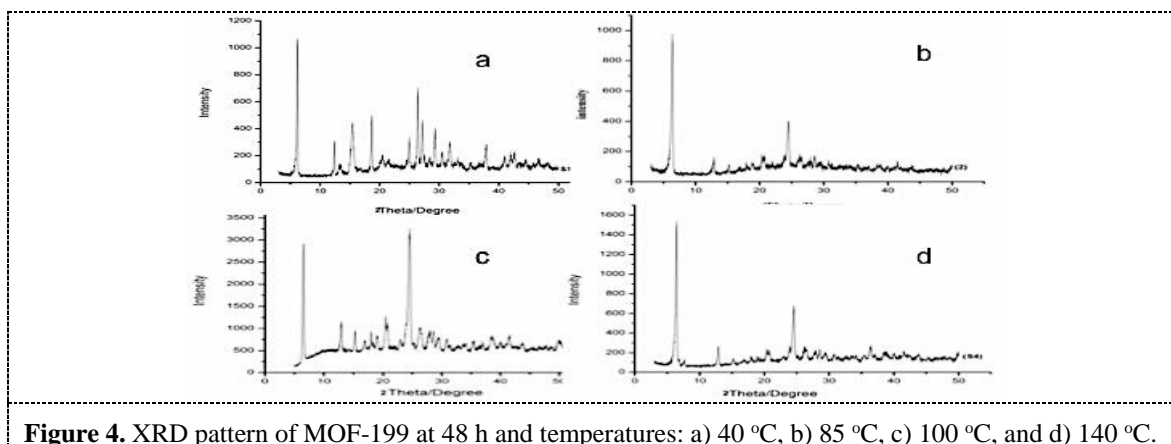
**Figure 2.** XRD pattern MOF-199 at  $T=100^{\circ}\text{C}$  for a) 18 h, b) 24h, c) 30h, and d) 48h.

Figure 3 illustrates the effect of increasing ethanol content in solvent volume for samples S6 and S8 in which all the synthesis conditions for both of these samples were practically the same except the  $\text{C}_2\text{H}_5\text{OH}:\text{H}_2\text{O}$  ratio were increased from 1:1 in sample S6 to 2:1 in sample S8. The Diffractogram data of crystals synthesized obtained with different solvent volume show the same typical pattern of MOF-199. However, decreases with the increase in  $\text{C}_2\text{H}_5\text{OH}:\text{H}_2\text{O}$  ratio shows decreasing in MOF-199 crystallinity (Table 2) which indicates that the best solvent ratio in at  $100^{\circ}\text{C}$  was 1:1  $\text{C}_2\text{H}_5\text{OH}:\text{H}_2\text{O}$  ratio.



**Figure 3.** XRD pattern of MOF-199 at  $100^{\circ}\text{C}$ , 48, and ;a) 1:1  $\text{C}_2\text{H}_5\text{OH}:\text{H}_2\text{O}$ , b) 2:1  $\text{C}_2\text{H}_5\text{OH}:\text{H}_2\text{O}$

XRD pattern of MOF-199 synthesized for 48 hours and at different heating temperatures ( $40$ ,  $85$ ,  $100$ , and  $140^{\circ}\text{C}$ ) are shown in Figure 4. For 48 h reaction time, the MOF-199 crystals have started to appear at  $40^{\circ}\text{C}$  as indicated by the presence of characteristic peaks of MOF-199 at  $2\theta = 6.5^{\circ}$ , and  $13.4^{\circ}$ . The MOF-199 is fully formed at heating temperatures of  $85^{\circ}\text{C}$  as can be identified by peaks characteristic to MOF-199. As can be shown in Figure 5, the obtained MOFs with reaction times of  $85$ – $140^{\circ}\text{C}$  have the same XRD pattern to that of typical MOF-199 in the literature [4]. However, the main peaks intensity increased with the increase in heating temperature from  $40$ – $100^{\circ}\text{C}$  and when increasing the temperature to  $140^{\circ}\text{C}$  the main peaks intensity were decreased.



**Figure 4.** XRD pattern of MOF-199 at 48 h and temperatures: a) 40 °C, b) 85 °C, c) 100 °C, and d) 140 °C.

These results have been confirmed by calculating the crystallinity of the MOFs (Table 2), which indicates that the MOF-199 crystallinity decreases with the overheating temperature for that reaction time. The crystallinity results and the BET surface area results are listed in Table 2. Therefore, based on the crystallinity of the obtained crystals and the XRD pattern for all synthesized samples, the crystallinity of samples S5 was the highest crystallinity. Nevertheless, from a comparison of the crystallinity for the XRD of MOF-199 and the BET surface area results, it is seen that the highest surface area (5518 m<sup>2</sup>/g) with high crystallinity off 103% was for S6 sample. Therefore, the optimum solvothermal for the synthesis of MOF-199 for the chosen operation conditions have chosen to be at 100 °C and 48 h. The solvothermal conditions are chosen based on the XRD patterns of the MOFs follow the pattern of typical XRD of MOF-199 with the high crystallinity and the highest surface. The surface area of prepared MOFs that was measured by physical nitrogen adsorption at liquid nitrogen temperature using the BET method. An increase in the surface area generally increases the catalyst activity [9]. The obtained value of the surface area of prepared MOF-199 in this research, is higher than the value obtained by Jiang (1247m<sup>2</sup>/g ,100 °C, 13 h) [8].

Figure 5 a and b shows representative morphology pictures of optimum synthesized MOF-199 for samples synthesized with reaction time 48 h at 85 °C and 100 °C, respectively. SEM characterization shows are in good agreement with the result obtained by Nobar [4].

**Table 2.** Summary of the Surface area and Crystallinity of MOF-199 samples

Sample	Time (h)	Temperature (°C)	Surface area m <sup>2</sup> /g	Crystallinity %
S1	18	100	1835	102
S2	24	100	2902	100
S3	30	100	3635	100
S4	48	40	NoMOF-199	NoMOF-199
S5	48	85	2679	106
S6	48	100	5518	103
S7	48	140	1059	63
S8	48	100	-	94

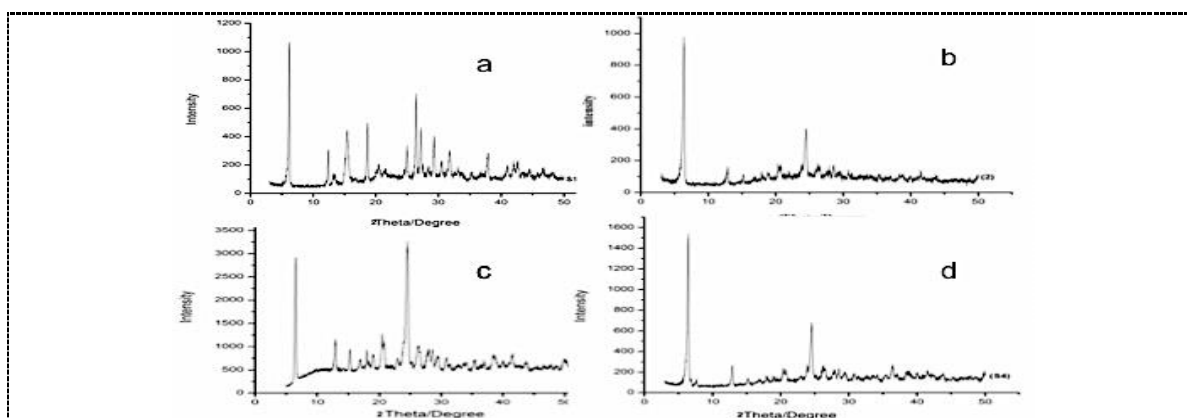


**Figure 5.** SEM images of synthesized MOF-199 samples at a). 24 h and 85°C, and b). 48 h and e 100°C

### 3.2. CO<sub>2</sub> adsorption on MOF-199

Carbon dioxide adsorption and desorption isotherms were measured on the optimum sample that was synthesized at 100 °C for 48 h (S6). The BET specific surface areas and pore volumes were calculated as 5518 m<sup>2</sup>.g<sup>-1</sup> and 0.609 cm<sup>3</sup>.g<sup>-1</sup>, respectively, Figure 6 presents the relation between amount of CO<sub>2</sub> adsorption *q* (mmol/g) and gas phase concentration equilibrium (*C<sub>e</sub>*)

The experimental adsorption isotherms of CO<sub>2</sub> on to MOF-199 was measured overpressure range (0-5 bar) at (36, 40, 60, 70 °C) as shown in Figure 6. the adsorption capacity on MOF-199 decrease with increase in temperature. In this study obtained a high adsorption capacity equal to 4.9 mmol/g at 5 bar, 36 °C. The effect of temperature on adsorption isotherm for carbon dioxide on MOF-199 (S6). From this Figure, it is seen that by increasing the equilibrium adsorption temperature the total amount of adsorbed on

S6 samples decreasing. With increasing temperature, the CO<sub>2</sub> adsorbed on MOF-199 surface becomes unstable because molecular diffusion increased that lead to more desorption of CO<sub>2</sub> molecules. This behavior has also been mentioned by [4]. Also the adsorption capacities in this study is in good agreement Zenga, who reported to obtaine 4 mmol/g at 1bar at 25 °C [2].

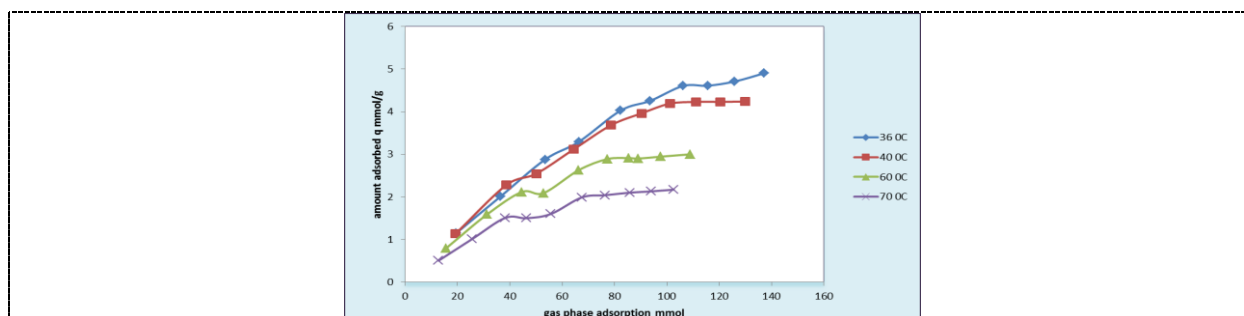


**Figure 6.** Adsorption equilibrium isotherm of carbon dioxide on MOF-19

## 4. Conclusions

From the experimental results, it has been concluded that the MOF-199 has been successfully synthesized at the optimal conditions of 100°C for 48 h. The synthesized sample MOF-199 value of the surface area (BET = 5518 m<sup>2</sup> g<sup>-1</sup>) porous size of crystal 11.8 Å, the specific volume 0.693 cm<sup>3</sup> g<sup>-1</sup> with high crystallinity of 103. The synthesized MOF-199 should be considered as an effective adsorbent for CO<sub>2</sub> with dioxide storage capacity of the 4.9 m<sup>2</sup> g<sup>-1</sup> at the pressure of 5 bar at 36 °C.

## References

- [1] Cui, P., Wu, J., Zhao, X., Sun, D., Zhang, L., Guo, J., and Sun, D. 2011 *Two solvent-dependent zinc (II) supramolecular isomers: rare kgd and lonsdaleite network topologies based on a tripodal flexible ligand*. (Crystal Growth & Design) vol 11(12) p 5182-5187.
- [2] Zeng, M., Wang, T., Liu, Y., Long, Z., and Sun, C. 2018 *Research on Planning Method of Microgrid Energy Unit in Intelligent Districts Containing Electric Vehicles Considering CO<sub>2</sub> Emission* (Chemical Engineering Transactions) vol 66 p 1339-1344.
- [3] Wang, X. 2017 *Computer Simulation and Process Improvement of CO<sub>2</sub> Capture by Chemical Absorption* (Chemical Engineering Transactions) vol 59 p 547-552.
- [4] Nobar S.N., 2012, *Adsorption and diffusion of gases in Cu-BTC*, (PhD Thesis, Sharif University of Technology Tehran, Iran).
- [5] Xie, J., Yan, N., Qu, Z., and Yang, S. 2012 *Synthesis, characterization and experimental investigation of Cu-BTC as CO<sub>2</sub> adsorbent from flue gas* (Journal of Environmental Sciences) vol 24(4) p 640-644.
- [6] Schlichte, K., Kratzke, T., and Kaskel, S. 2004 *Improved synthesis, thermal stability and catalytic properties of the metal-organic framework compound Cu<sub>3</sub> (BTC) 2* (Microporous and Mesoporous Materials) vol 73(1-2) p 81-88.
- [7] Lin, K. S., Adhikari, A. K., Ku, C. N., Chiang, C. L., and Kuo, H. 2012 *Synthesis and characterization of porous HKUST-1 metal organic frameworks for hydrogen storage* (international journal of hydrogen energy) vol 37(18) p 13865-13871.
- [8] Jiang, D., Mallat, T., Krumeich, F. and Baiker, A. 2011 *Polymer-assisted synthesis of nanocrystalline copper-based metal-organic framework for amine oxidation*. (Catalysis Communications) vol 12(7) p 602-605..
- [9] Rallan Ch.A., AlRubaye R.Th. and Garforth A.A. 2015 *Generation of Catalytic Films of Alumina and Zeolites on FeCralloy Rods* (Chemical Engineering Transactions) vol 43 p 907-913.